Colloidal Quantum Dot Sensor Bandwidth and Thermal Stability: Progress and Outlook

White Paper

ABSTRACT

Shortwave IR (SWIR) sensors made using colloidal quantum dot photodiodes offer CMOS-like opportunities for highly scalable, small pixel pitch sensors, owing to their straightforward, monolithic integration with silicon circuitry. SWIR Vision Systems began to realize this potential when it introduced its 2.1 MP Acuros cameras to the industrial, scientific, and commercial imaging markets in 2018. Other opportunities for this detector technology can be found in the need for new sensor technologies in the development of cost and resolution scalable direct time of flight depth sensing systems for consumer and automotive applications. But to realize this potential, this relatively new detector system must also be shown to meet thermal and environmental conditions found in consumer and automotive devices. This paper will provide an overview of the performance of our high definition sensors; and show <3 ns rise/fall time results from testing the response time of the photodiode structure using a pulsed laser sources. It will also present data demonstrating stable device operation at elevated temperature and humidity conditions.

Keywords: Colloidal Quantum Dot Sensors, Shortwave infrared, SWIR, CQD, SWIR Image Sensors, SWIR Focal Plane Arrays, NIR Image Sensor

SWIR Vision Systems
www.swirvisionsystems.com
sales@swirvisionsystems.com

SWIR Colloidal Quantum Dot Sensor Bandwidth and Thermal Stability: Progress and Outlook

C. Gregory, J.A. Hilton, K. Violette, S. Shefte, C. Procida, T. Tewodros, M. Bond, E.J.D. Klem[a]
[a]SWIR Vision Systems, 3021 Cornwallis Rd, Durham, NC, USA 27709

ABSTRACT

Shortwave IR (SWIR) sensors made using colloidal quantum dot photodiodes offer CMOS-like opportunities for highly scalable, small pixel pitch sensors, owing to their straightforward, monolithic integration with silicon circuitry. SWIR Vision Systems began to realize this potential when it introduced its 2.1 MP Acuros cameras to the industrial, scientific, and commercial imaging markets in 2018. Other opportunities for this detector technology can be found in the need for new sensor technologies in the development of cost and resolution scalable direct time of flight depth sensing systems for consumer and automotive applications. But to realize this potential, this relatively new detector system must also be shown to meet thermal and environmental conditions found in consumer and automotive devices. This paper will provide an overview of the performance of our high definition sensors; and show <3 ns rise/fall time results from testing the response time of the photodiode structure using a pulsed laser sources. It will also present data demonstrating stable device operation at elevated temperature and humidity conditions.

Keywords: Colloidal Quantum Dot Sensors, Shortwave infrared, SWIR, CQD, SWIR Image Sensors, SWIR Focal Plane Arrays, NIR Image Sensor

1. SENSOR AND CAMERA PERFORMANCE

1.1 Introduction

SWIR Vision Systems' direct-deposited, thin-film photodiode array technology uses a colloidal quantum dot broadband absorber with a band-gap that can be tuned during colloidal quantum dot synthesis across the spectral range from the near infrared (NIR) to the extended shortwave infrared (eSWIR). Today, SWIR Vision Systems produces cameras with visible (Vis)-SWIR response from 400 to 1650 nm and a Vis–eSWIR sensitivity camera with response from 350 to 2100 nm. The processes used to deposit the materials for the diode are all processes that are found in standard CMOS wafer processing. Owing to the monolithic integration of the colloidal quantum dot photodiode array, the low cost of colloidal quantum dot solution synthesis, and the large area deposition processes used in their fabrication, colloidal quantum dot photodiode arrays offer a straightforward path for fabricating large format FPAs at the wafer scale.

.

1.2 Quantum Efficiency

SWIR Vision Systems' standard SWIR image sensors are fabricated using colloidal quantum dot material with a first excitonic peak at approximately 1500 nm. The spectral response of these sensors follows the optical absorption properties of the colloidal quantum dot material, which, like traditional semiconductor materials, contain a density of electronic states above the optical bandgap, enabling photon absorption from the SWIR down to UV wavelengths. Figure 1 shows the spectral response of the standard SWIR image sensor.

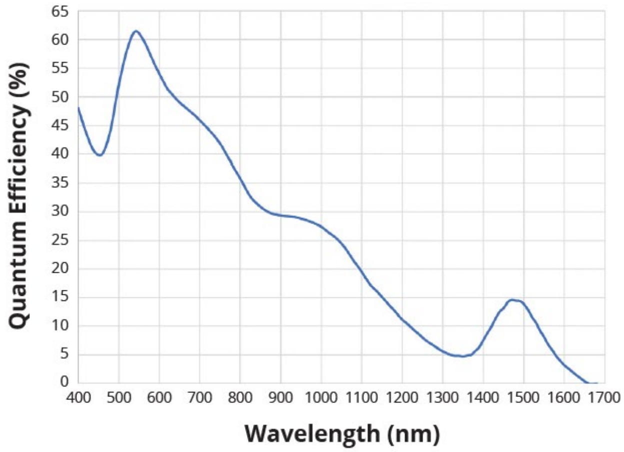

Figure 1. Spectral response of the standard SWIR image sensors being offered today commercial Acuros® camera products

One should note that the quantum efficiency (QE) of the CQD® diodes is lower than traditional SWIR InGaAs-based sensors. However, this is not a fundamental limit of the CQD material system, and development efforts to increase the QE performance are bearing fruit.

1.3 Sensor Noise

To produce focal plane arrays and cameras, CQD photodiodes are fabricated on the surface of read out ICs (ROICs) which contain an array of amplifiers, multiplexing circuitry, and other functions needed to produce a digital image. In the SWIR Vision System's commercial Acuros product line the ROIC is a 15 µm pitch design and contains three analog gain modes corresponding to three different full well capacities of 550 ke-, 110 ke-, and 25 ke-. The sensors feature a global snapshot shutter and full frame rates of 60 fps for the HD sensor.

The read noise performance of the sensor is reduced by the implementation of a correlated double sampling architecture in the ROIC. The dark current of our CQD diode structure is about 5 nA/cm^2 at 25C which starts to be a significant contributor to total system dark noise for exposure times greater than about 20 ms. Below these exposure times, the dark noise performance is dominated by the ROIC read noise. A summary table showing the performance of the Acuros 1920 camera under different operating modes can be seen in Table 1.

Table 1. Summary of the Acuros 1920 Camera Performance in each of its three analog gain modes

	Full Well Capacity	Total dark noise per pixel (Note 1)	Noise Equivalent Power (Note 2)	Dynamic Range
Low Gain	550 ke-	183 e-	12 nW/cm^2	70 dB
Med Gain	110 ke-	76 e-	5 nW/cm^2	67 dB
High Gain	25 ke-	65 e-	4 nW/cm^2	32 dB

Note 1: Total input referred dark noise measured at a sensor operating temperature of 30 C and 16.6 ms exposure time.
Note 2: Measured using 1550 nm illumination and 16.6 ms exposure time with a 30 C sensor temperature.

1.4 Acuros Extended SWIR Cameras

SWIR Vision Systems has released a series of cameras with a spectral response spanning 350 nm to 2100 nm. These cameras share a common feature set with the standard Acuros cameras with the same resolution options, well depths, and camera features. The extended SWIR photodiodes that SWIR Vision System builds for these sensors have room temperature dark current densities in the 5 nA/cm^2 range. This leads to excellent noise performance without the deep cooling found in traditional extended SWIR cameras made with InSb, HgCdTe, or Type II Superlattice detectors. A plot of the responsivity of the eSWIR cameras can be seen in Figure 2.

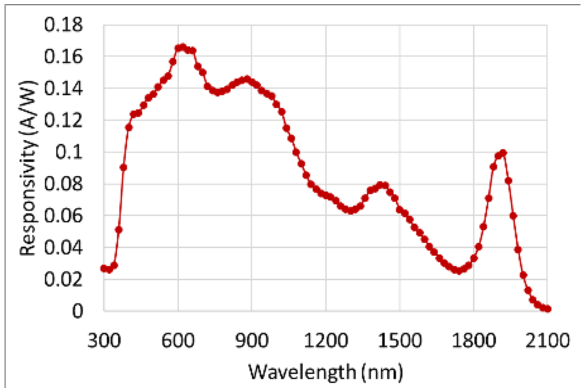

Figure 2. Spectral response of the Acuros eSWIR cameras

1.5 Increasing photodiode QE

The quantum efficiency of CQD-based photodiodes has typically lagged behind that of traditional CMOS and InGaAs detectors. This is primarily a function of the incomplete optical absorption that occurs in the relatively thin films used to fabricate CQD detectors. Increasing the QE by increasing the CQD film thickness is challenged by the short charge transport lengths found in the ensemble of nanometer-scale crystal domains formed in CQD films. The SWIR Vision Systems team has worked to improve the QE of the CQD detectors by focusing on the underlying physics of charge transport within the CQD films. Indeed, one of the great opportunities for improvements in CQD device performance lies in the ability to control the electronic properties of CQD films through the manipulation of the chemical properties of individual dots. Utilizing this characteristic, the SWIR Vision team has made strides in producing higher QE detectors. The team has made enhanced QE photodiodes on test arrays and has characterized their spectral response, dark current, and other performance characteristics. The spectral response of one of these devices with a first excitonic peak at approximately 1500 nm can been seen in Figure 3.

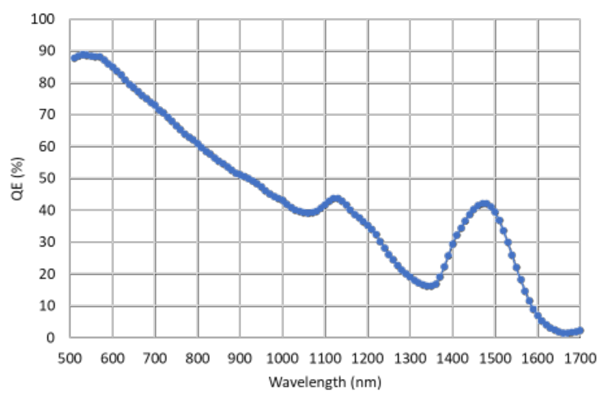

Figure 3. Quantum efficiency spectrum of enhanced QE CQD photodiodes demonstrated on small pixel array test devices. The dark current density for this device was measured to be 8 nA/cm2 at 25C.

2. DEMONSTRATION OF DIRECT TIME OF FLIGHT DISTANCE MEASUREMENT

Depth sensing systems utilizing active optical sources and optical detectors to determine the three dimensional structure and distance of objects from the system and within a scene are useful in applications in industrial, scientific, consumer, automotive and security markets. A shortcoming of current approaches to building these systems is a lack of a scalable detector structure capable of performing high speed detection in the SWIR spectral regions.

To demonstrate the utility of colloidal quantum dot detector-based optical depth sensor system, a colloidal quantum dot photodiode was used to measure the rise and fall time characteristics of a laser pulse. Figure 4 shows a diagram of the apparatus and setup used for this measurement. In it, a Nd:YAG (Neodymium doped Yttrium Aluminum Garnet) pulsed laser emits a series of laser pulses which travel through the air to illuminate a colloidal quantum dot photodiode detector and an InGaAs photodiode that is used as a reference detector. The Nd:YAG laser has a 3-5 ns full-width half-maximum pulse width and is configured to operate at a 5 Hz repetition rate. The colloidal quantum dot photodiode is a 0.2 mm x 0.2 mm square detector whose electrical output is connected to an oscilloscope (Agilent part number MSO8104A). The InGaAs reference photodiode is a 0.15 mm diameter detector (Thorlabs part number FGA015) whose output is also connected to the oscilloscope and is used as the trigger source for the oscilloscope measurements.

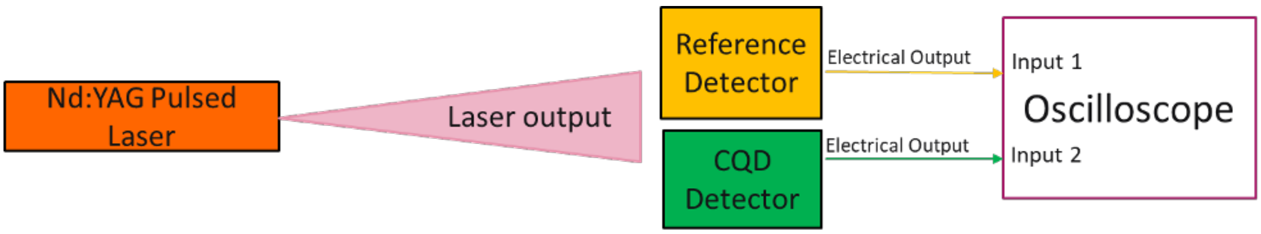

Figure 4. Diagram showing apparatus and setup used in CQD photodetector response time measurement

The data collected during this measurement is shown in Figure 5. In it, a screen shot of the oscilloscope display shows the output of the InGaAs photodiode reference detector and the colloidal quantum dot photodiode. During this measurement the oscilloscope was configured to measure the 10%-90% rise times and the 90%-10% fall times for the reference detector and the colloidal quantum dot detector. The mean rise/fall times along with additional measurement statistics are also shown in Figure 5. This measurement data was reported by the oscilloscope. It shows that the colloidal quantum dot detector had a mean rise time of 1.01 ns and a mean fall time of 2.79 ns. Both the rise and fall times were shorter than that measured using the InGaAs reference detector and therefore likely represent the limits achievable with the laser source and not the rise and fall time limits of the colloidal quantum dot detector architecture and optical depth measurement system.

The measurement of rise and fall times less than 3 ns from the colloidal quantum dot detector shows that it has the time response characteristics needed for depth sensing systems.

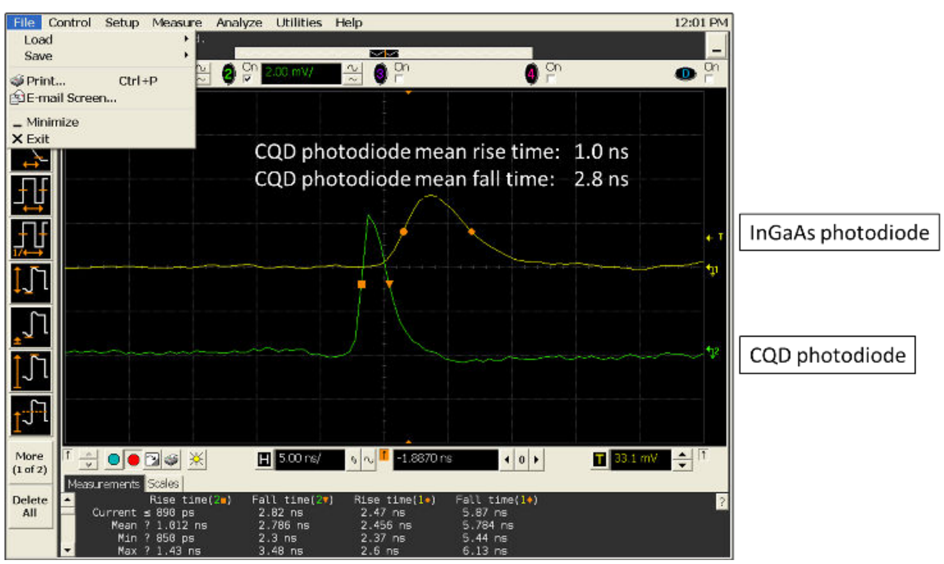

Figure 5. Image of oscilloscope screen shots taken during CQD photodiode response time measurement

To carry out a demonstration of a colloidal quantum dot detector optical depth measurement system, a setup shown in Figure 6 was assembled. In this two-part measurement a laser pulse was used to illuminate a piece of white, opaque plastic. The laser pulse then reflected off the plastic and the reflected light was detected by both a reference detector and colloidal quantum dot detector whose electrical outputs were measured by an oscilloscope. The detectors and oscilloscope used for this measurement were the same as that used in the Figure 4 and Figure 5 measurements.

In part one of the measurement the reference detector and the colloidal quantum dot detector were co-located the same distance from the reflective white plastic surface. In part two of this measurement the colloidal quantum dot detector was moved to be 28 cm from the reference detector position. This resulted in a 28 cm path-length difference for the optical pulse to travel before being detected by the colloidal quantum dot detector.

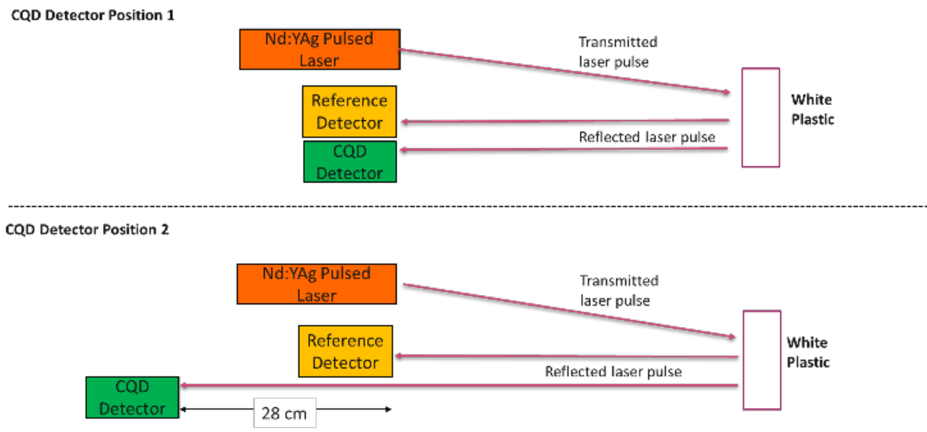

Figure 6. Diagram of setup used in demonstration of CQD detector optical distance sensor

Figure 7 shows screen shots taken of the colloidal quantum dot and reference detector electrical output in position 1 and position 2. In position 1, the detectors are co-located. In position 2 the detectors are 28 cm apart. The time difference between the 50% signal level on the rising edge of the two detector outputs was measured using the oscilloscope for both detector positions. The change in the arrival time difference between the two measurements was 0.94 ns. This 0.94 ns shift in pulse arrival time arose because the distance the light pulse had to travel through free-space was increased by 28 cm between the two measurements.

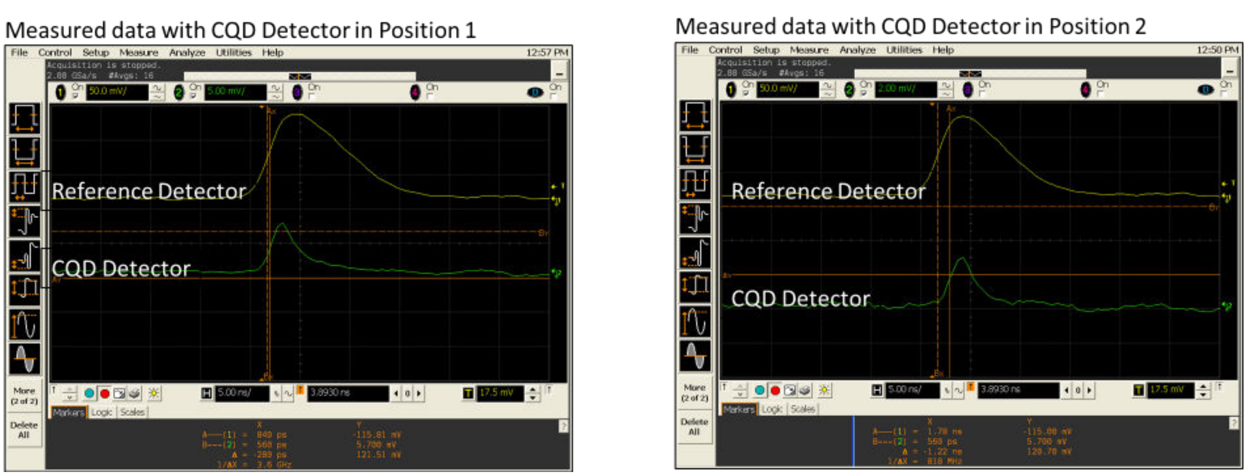

Figure 7. Images of oscilloscope screen shots taken during CQD photodetector optical distance sensor demonstration. Notes: 1) CQD detector position is changed between two measurements. Reference detector

position is fixed. 2) 28 cm physical separation between CQD and Reference when CQD detector is in Position 2. 3) 0 cm physical separation between CQD and Reference detector when CQD detector is in Position 1. 4) 0.94 ns change in pulse arrival time at CQD detector between two measurements

Using the velocity of light in air one can calculate that in 0.94 ns the optical pulse is expected to travel 28.2 cm. This corresponds well to the measured change in optical path length of 28 cm. Accordingly, these measurements show that an optical depth sensing system with colloidal quantum dot detectors can be implemented to measure distance in direct time of flight 3D depth sensing.

3. THERMAL STRESS TESTING OF CQD DEVICES

For CQD sensors to be used in high volume automotive and consumer applications, they will need to be built to the storage and operating temperature specifications found within those applications. To meet this requirement, SWIR Vision has been fabricating sensors and stress testing them in high temperature and high humidity environmental stress test chambers. One set of data generated during this testing can been seen in Figure 8.

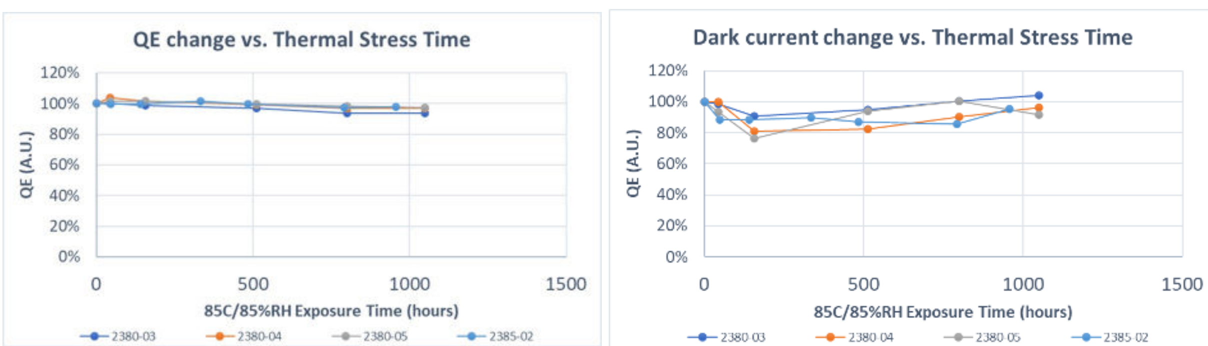

Figure 8. Photodiodes exposed to 85C/85% RH storage conditions. QE (1550 nm illumination) and dark current collected periodically during testing. Data shows stable performance for these environmental conditions over the >1000 hours tested.

Figure 8 illustrates change in sensor dark signal and photoresponse as a function of thermal stress time for CQD photodiodes fabricated in test arrays consisting of 200 x 200 um and 1 x 1 mm detectors on silicon fanout die. Figure 9 illustrates the thermal stability of a set of 1920 x 1080 format, 2.1 megapixel image sensors. The plotted data of Figure 9 illustrates the mean dark signal of each pixel array normalized to the time zero data point. It shows measured data collected at different times as the sensors 1, 2, 3, 4, 5 and 6 were exposed to 75°C, 85% relative humidity conditions in a stress test chamber. Fig. 9 also shows the mean photoresponse for the same sensors 1, 2, 3, 4, 5 and 6 as a function of stress test chamber exposure time.

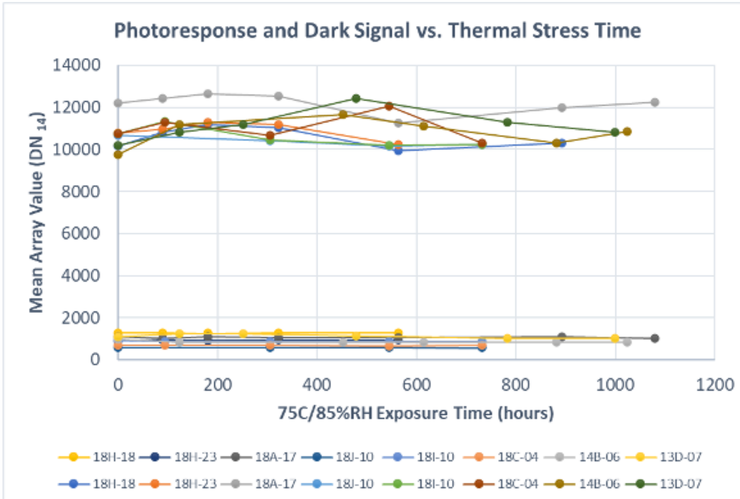

Figure 9. HD sensors exposed to 75C/85% RH storage conditions. Photoresponse (1550 nm light) and dark signal collected periodically during testing.

This stress data indicates that the diode structure and packaging solution developed by SWIR Vision show stable sensor performance for conditions needed for many consumer electronics applications. To meet the needs of automotive applications SWIR Vision has also initiated 105 C stability testing with preliminary data showing similarly stable performance as that observed at lower temperatures.

4. OUTLOOK AND PROSPECTS FOR CQD SENSORS AND DETECTORS

In summary, we have presented an overview of the CQD detector technology that SWIR Vision Systems offers in its family of high resolution SWIR and eSWIR cameras. These cameras are being utilized for applications including laser profiling, semiconductor inspection, long range outdoor imaging, and other machine vision applications. We have shown results of work advancing the properties of the CQD detectors and report prototype demonstrations of high QE detectors (1550 nm QE = 45%). We have also shown that the CQD photodiode structure developed by SWIR Vision Systems is capable of supporting sub 5 ns optical pulse measurements with rise and fall times in 200 um x 200 um devices measured to be 1 and 3 ns respectively. This bandwidth performance is sufficient for direct time of flight systems where a need exists for detector technologies capable of scaling to the pixel pitch and price points required for consumer and automotive systems. Finally, we show progress on increasing the high temperature and humidity environmental specifications for these sensors and report stable operation after >1000 hours at 85 C and 85% relative humidity.

Table 2. Summary of SWIR Vision Photodiode Performance Parameters

Metric	**Value**	**Notes/Measurement Structure**
Photodiode structure	Type-II photodiode	*pn* junction using PbS CQDs capable of photovoltaic operation
Bandwidth	>350 MHz	1 ns rise time and 3 ns fall time measured on 200 um x 200 um test diodes. Enables Direct ToF 3D depth sensing
Dark current	<5 nA/cm^2, 25 C	Typical dark current density measured on 15 um pixels in 2MP image sensors and on 200 um x 200 um test diodes
Quantum Efficiency	15% to 45% at 1550 nm depending on diode type	See spectral QE plots in following slides for details. Bandgap of detectors can be selected during fabrication to match system requirements.
Bias Voltage	<0.1 V	Reverse bias voltage typically used in 2MP image sensors and 200 um x 200 um test diodes
Capacitance	<15 pF	Measured using 200 um x 200 um test diodes
Linearity	< +/-1.5% deviation	Evaluated on 2MP image sensors using array response to 1550 nm light source
Pixel Yield	> 99.95% typical > 99.90% min	Evaluated on 2MP image sensors. Bad pixels are those with light or dark response >+/-25% of mean array response
Commercial availability	Yes	Acuros family of CQD sensors and cameras shipping globally since 2018